Reprint

J.M. Costa, A.N. Venetsanopoulos and M. Trefler, "Design and implementation of digital tomographic filters", *IEEE Transactions on Medical Imaging*, Vol. MI-2, No. 2, pp. 89-100, June 1983.

Design and Implementation of Digital Tomographic Filters

JOSÉ M. COSTA, ANASTASIOS N. VENETSANOPOULOS, AND MARTIN TREFLER

Abstract—A technique is proposed which allows the selective filtering of conventional radiographs in order to obtain depth-dependent information by utilizing the depth-dependent information contained therein. This technique, referred to as tomographic filtering or tomographic filtration process (TFP), takes advantage of the finite size of the X-ray source, so that after processing, the image of a particular layer is improved while the others are not. This paper starts with a brief review of technique and then concentrates on the design and implementation of digital tomographic filters. Examples are shown, including images of simulated radiographs processed with such filters. Evaluations of the performance of these filters show that the image quality cannot be as good as that of standard tomography or multiprojection reconstruction techniques; nevertheless they represent an improvement over conventional radiology, and highlight additional depth-dependent information contained in radiographs. This paper concludes with suggestions for further research in this area.

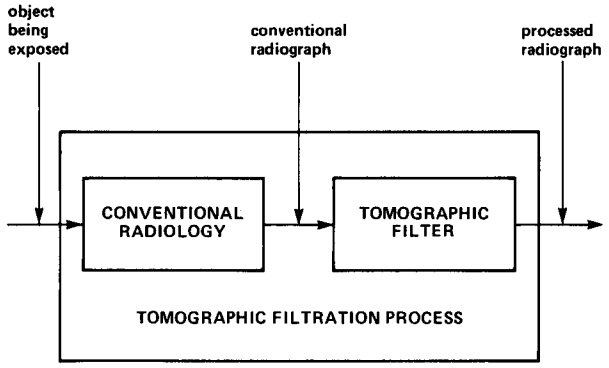

Fig. 1. Conceptual difference between "tomographic filtering" and a "tomographic filtration process" (TFP).

I. Introduction

RECENTLY, a technique has been proposed which allows the processing of conventional radiographs in order to obtain information about the depth of details and structures [1]-[5]. This technique takes advantage of the finite size of the X-ray source and the divergent nature of the X-ray beam, which results in a radiograph that contains depth-dependent information. By selective filtering of the radiograph, it is then possible to obtain an improvement of the image of a particular layer while the others are degraded. This technique has been referred to as tomographic filtering or a tomographic filtration process (TFP). While tomographic filtering usually refers to the filter that produces tomographic restoration, the term TFP refers to the complete system, including the conventional radiography equipment[1] (Fig. 1). The objective of this paper is to discuss the design and implementation of digital tomographic filters and to present some of the practical results that have been obtained. The mathematics of tomographic filtering have appeared elsewhere [1]. Tomographic filtering has also been evaluated from an analytical viewpoint by comparing this technique with standard tomography and conventional radiography [2], [3]. Tomographic filtering is briefly reviewed in Section II. The design of digital tomographic filters is covered in Section III. Implementation and examples of application are given in Section IV. Conclusions and suggestions for further research appear in Section V.

II. Tomographic Filters

Tomographic filtering takes advantage of the depth-dependent blur, which is due to the finite dimensions of the focal spot. This is better understood by comparing it with standard tomography.

Standard tomographic techniques produce a tomogram by moving a point-like X-ray source and the recording film in a coupled manner. The movement is done in such a way, that during the exposure only parts of the body lying in one specific plane parallel to the film plane are always projected on the same place on the film, while the others are blurred [1], [3]. The layer whose image is in focus is referred to as the plane of cut or tomographic layer.

Tomographic filters produce a focusing effect similar to that of standard tomography; but with no moving parts. With tomographic filters, instead of moving the X-ray tube, the finite size of the focal spot is used to advantage and instead of moving the film, a filter is used to process a conventional radiograph. Indeed, by moving a hypothetical point source over the region of the actual source, and applying superposition, we can model a distributed source of X-rays[2]. Since in conventional radiography the film does not move, the images

Manuscript received March 16, 1983; revised July 28, 1983.

J. M. Costa is with Bell-Northern Research, Ottawa, Ont., Canada K1Y 4H7.

A. N. Venetsanopoulos is with the Department of Electrical Engineering, University of Toronto, Toronto, Ont., Canada M5S 1A4.

M. Trefler is with the Department of Radiology, Division of Radiological Sciences, School of Medicine, University of Miami, Miami, FL 33101.

[1]Notice that the two terms are often used interchangeably and it is usually clear from the context what is meant. Throughout this paper we will generally use tomographic filtering.

[2]The movement of this point source is analogous to the movement of an X-ray tube in standard tomography.

0278-0062/83/0600-0089$01.00

of all the layers are blurred. Therefore, in order to convert a radiograph into a tomogram the radiographic image is processed by a filter that will produce an effect equivalent to that produced by the motion of the film in standard tomography.

To illustrate this, consider Fig. 2. Suppose that the tomographic layer is at a distance Δ_1 from the focal spot S and at a distance Δ_2 from the film plane. If 0 is a point on the tomographic layer, its image on the film extends over a distance U as shown in Fig. 2. This blur U is the one that we want to eliminate[3]. All other blurs corresponding to other layers, such as the blur V of the point X and the blur V' of the point X', differ in size and therefore, cannot be eliminated simultaneously. The extension to two dimensions is straightforward.

The equations of tomographic filtering have been derived in detail in [1]. The results show that the equations of image formation in standard tomography, conventional radiology, and tomographic filtering are similar.

The frequency domain equation of image formation in radiology is

$$G(f_x, f_y) = I_B\,\delta(f_x, f_y) - \int_0^d H_i(f_x, f_y, z_i) \cdot F_\mu(f_x, f_y, z_i)\,dz_i \tag{1}$$

where $G(f_x, f_y)$ is the Fourier transform of the resulting image, I_B is a constant, $\delta(f_x, f_y)$ is the Dirac delta function, $H_i(f_x, f_y, z_i)$ is the overall transfer function of the ith layer at a depth z_i, and $F_\mu(f_x, f_y, z_i)$ is the Fourier transform of the (scaled) distribution of linear absorption coefficients $\mu(x, y, z_i)$ in the ith layer (cf. [1]).

Equation (1) is general and it applies to standard tomography, conventional radiology and tomographic filtering by using the overall transfer function given in (2), (3), or (4), respectively (cf. [1]).

Standard Tomography:

$$H_i^{ST}(f_x, f_y, z_i) = \left[\frac{z_i - d}{z_i - \Delta_2}\,\frac{\Delta_1}{d}\right]^2 \cdot \iint I_o\left\{\frac{z_i - d}{z_i - \Delta_2}\,\frac{\Delta_1}{d}\,x, \frac{z_i - d}{z_i - \Delta_2}\,\frac{\Delta_1}{d}\,y\right\} \cdot e^{-j2\pi(f_x x + f_y y)}\,dx\,dy. \tag{2}$$

[3]Here we define blur as the extent of the image of a point or edge due to the finite size of the focal spot.

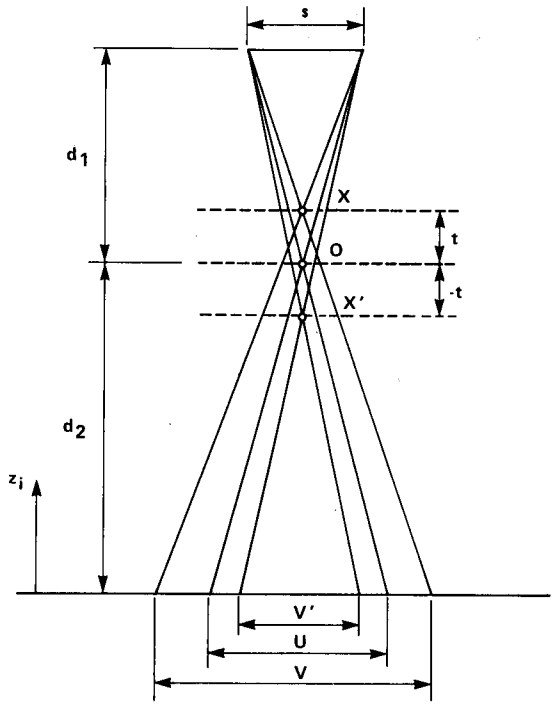

Fig. 2. Blur formation in the radiologic process.

Conventional Radiology:

$$H_i^{CR}(f_x, f_y, z_i) = \left[\frac{z_i - d}{z_i}\right]^2 \iint I_o\left\{\frac{z_i - d}{z_i}\,x, \frac{z_i - d}{z_i}\,y\right\} \cdot e^{-j2\pi(f_x x + f_y y)}\,dx\,dy. \tag{3}$$

Tomographic Filtering:

$$H_i^{TF}(f_x, f_y, z_i) = \frac{\left[\frac{z_i - d}{z_i}\right]^2 \iint I_o\left\{\frac{z_i - d}{z_i}\,x, \frac{z_i - d}{z_i}\,y\right\} e^{-j2\pi(f_x x + f_y y)}\,dx\,dy}{H(f_x, f_y)} \tag{4}$$

where

$$H_t(f_x, f_y) = \frac{1}{H(f_x, f_y)} = \frac{1}{H_i^{CR}(f_x, f_y, z_i)}\bigg|_{z_i = z_t} = \frac{1}{\left[\frac{z_t - d}{z_t}\right]^2 \iint I_o\left\{\frac{z_t - d}{z_t}\,x, \frac{z_t - d}{z_t}\,y\right\} e^{-j2\pi(f_x x + f_y y)}\,dx\,dy} \tag{5}$$

where the depth of the tomographic layer is $z_t \triangleq \Delta_2$, $d \triangleq \Delta_1 + \Delta_2$, and $I_o(.,.)$ is the exposure function, that is either the intensity distribution of the movement of an X-ray source in standard tomography or the focal spot X-ray distribution in conventional tomography and tomographic filtering [1]-[3]. Equation (5) shows that the transfer function of the tomographic filter $H_t(f_x, f_y)$ is the inverse of the transfer function for conventional radiology for $z_i = z_t$.

In spite of the fact that the equations of image formation in standard tomography, conventional radiology, and tomographic filtering are similar, there exist fundamental physical differences among these methods. A good objective indication of performance of a radiologic system is given by the overall

transfer functions of the layers in the object. The qualitative differences among these transfer functions were discussed in [1], while various quantitative performance parameters were examined in [2].

As shown in [1], of particular interest are the characteristics of the transfer function in (4) for tomographic filtering when the depth z varies. Indeed, for layers between the focal spot and the plane of cut this transfer function has low-pass characteristics, while between the plane of cut and the film has high-pass characteristics [1].

A comparative assessment of tomographic filtering has been produced from an analytical point of view[4] [2], [3]. A summary is given in [1]. These results show that tomographic filtering can be an improvement over conventional radiology, but cannot achieve the results of standard tomography.

III. Design of Tomographic Filters

The transfer function in (5) is to be applied to the radiological image represented by $G(f_x, f_y)$ in (1) (cf. [1])

$$F(f_x,f_y) \triangleq \frac{G(f_x,f_y)}{H(f_x,f_y)} = I_B \frac{\delta(f_x,f_y)}{H(f_x,f_y)} - \int_0^d \frac{H_i(f_x,f_y,z_i)}{H(f_x,f_y)} F_\mu(f_x,f_y,z_i)\,dz_i \qquad (6)$$

where $F(f_x, f_y)$ is the Fourier transform of the radiographic image after it has been processed with a tomographic filter.

In this section we examine the process of designing a digital filter with transfer function $H_t(f_x, f_y)$ as given by (5). The approach used is inverse filtering, which is not the best but the simplest. Three steps are considered: 1) determination of the function I_o, 2) noise handling technique, and 3) determination of the coefficients of the digital filter.

A. Determination of the Function I_o

In order to determine $H_t(f_x, f_y)$ as given by (5) the following information is needed:

1) the distance d between the focal spot and the film when the object is imaged,

2) the depth z_t of the layer of interest in the object that has to be deblurred, and

3) the exposure function $I_o(x_o, y_o)$.

The exposure function $I_o(x_o, y_o)$ can be obtained by imaging an object with a known distribution of absorption coefficients, such as a pinhole. The pinhole approximates a delta function and thus the system impulse response or point-spread function (PSF) $h(x, y)$ is obtained. It can easily be shown that

$$I_o(x_o,y_o) = h\left(\frac{d}{d_1}x_{io} - \frac{d_2}{d_1}x_o, \frac{d}{d_1}y_{io} - \frac{d_2}{d_1}y_o\right) \qquad (7)$$

[4]Tomographic filtering has been compared with standard tomography/zonography and conventional radiology on the basis of the following evaluation criteria: the exposure angle, the thickness of the cut, the rate of change of the transfer function, the signal-to-noise ratio, and the radiation dose [2], [3].

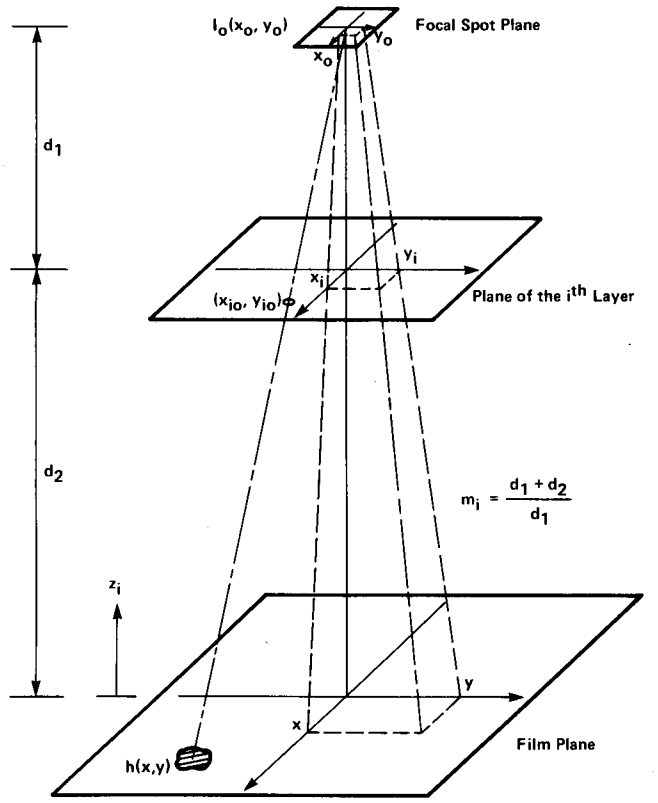

Fig. 3. Relationship between coordinates on different planes in the space-invariant model.

where (x_{io}, y_{io}), d_1 and d_2 determine the position of the pinhole[5], and $d = d_1 + d_2$ (cf. Fig. 3) [3], [6]-[8].

Actual PSF's were obtained using the pinhole method and the X-ray equipment of the Radiological Research Laboratories, University of Toronto. Contour and perspective plots of a typical PSF and its squared modulation transfer function (MTF) are shown in Fig. 4. The nominal size of this focal spot was 2 mm. The X-ray film was digitized and the squared MTF was calculated using a two-dimensional FFT [3].

As will be shown later, it is convenient to approximate the PSF by a separable function to save computer memory in the design of a tomographic filter. We have chosen a separable approximation in the frequency domain. Denote the PSF by $h(x, y)$ and its two-dimensional Fourier transform by $H(f_x, f_y)$. Then define a separable PSF $h_s(x, y)$ as

$$h_s(x,y) = h_x(x) \cdot h_y(y)$$

where

$$h_x(x) = \mathcal{F}^{-1}\{H_x(f_x)\} \triangleq \mathcal{F}^{-1}\{H(f_x,0)\}$$

$$h_y(y) = \mathcal{F}^{-1}\{H_y(f_y)\} \triangleq \mathcal{F}^{-1}\{H(0,f_y)\}.$$

The separable two-dimensional Fourier transform of $h_s(x, y)$ is then

$$H_s(f_x,f_y) = H_x(f_x) \cdot H_y(f_y) = H(f_x,0) \cdot H(0,f_y).$$

According to the projection-slice theorem [9], this approximation keeps the projections of the PSF along the x-axis and

[5]The notation d_1 and d_2 is used for any given layer, while the notation Δ_1 and Δ_2 is used exclusively for the plane of cut.

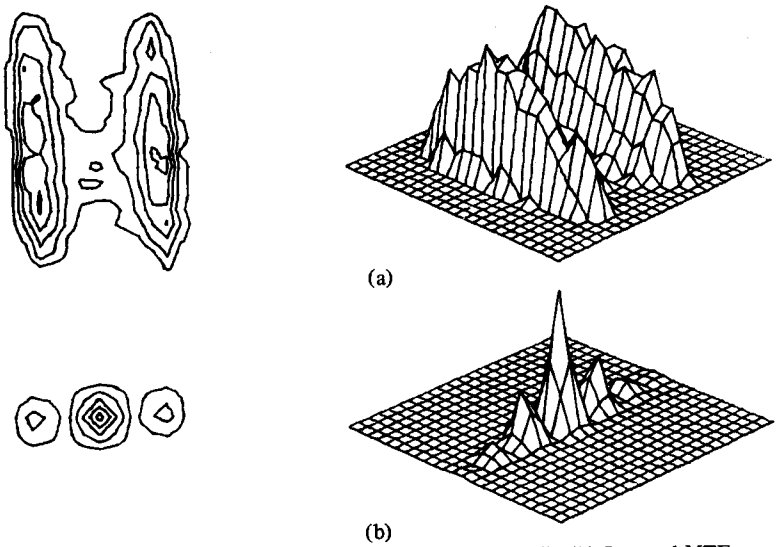

Fig. 4. Actual focal spot of 2 mm nominal size. (a) PSF. (b) Squared MTF.

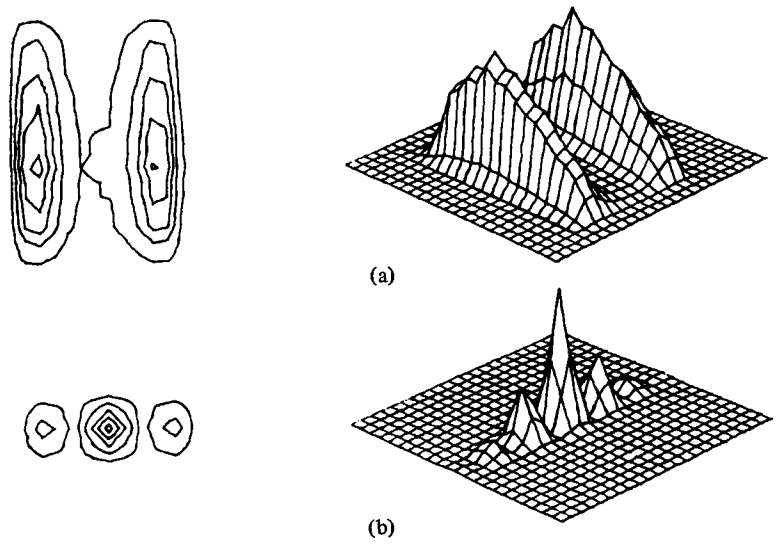

Fig. 5. Approximation of the focal spot in Fig. 5 by a separable function. (a) PSF. (b) Squared MTF.

y-axis invariant. This results also in further advantages, such as smoothing of the PSF and reduced computer time. The result of this approximation on the PSF's of Fig. 4 is shown in Fig. 5.

The transfer function $H_t(f_x, f_y)$ is then calculated according to (5) and can be implemented using digital (cf. [3]) or optical techniques (cf. [7], [8]). This paper deals with the digital implementation only.

It should be noted that the PSF $h(x, y)$ has to be measured only once for a given focal spot, because the tomographic filter transfer function $H_t(f_x, f_y)$ can be determined for any layer using the appropriate scaling factors [cf. (5) and (7)].

B. Noise Handling Technique

The filtering operation is indicated in (6). Unfortunately, $H(f_x, f_y)$ may have zeros and $G(f_x, f_y)$ is usually corrupted by noise. Thus the filtered image would include a large amount of noise at spatial frequencies in the neighborhood of a zero of $H(f_x, f_y)$. If the zeros are located at frequencies which are higher than those where the relevant physiological information is contained, a low-pass filter will be sufficient. Otherwise, noise handling techniques are necessary. Many such techniques have been described in the literature [10], [11]. No comparative assessment of all these techniques is available, but only subjective estimates in specific cases [12]. Inverse filtering is not the best (especially in the presence of noise), but it is the simplest. Since our goal was not the determination of the best method of image restoration, but to test the feasibility of tomographic filtering, we used a simple technique, which provides a means for hard-limiting the magnitude response of the inverse filter while preserving the phase response and cutting off the high frequencies dominated by noise. Both the hard-limit and cutoff frequency can be specified by the user.

We want to design a filter whose transfer function $\overline{H}_t(f_x, f_y)$ is a modified version of $H_t(f_x, f_y)$, as shown in (5), in order to satisfy the constraints:

1) the magnitude response is limited

$$|\overline{H}_t(f_x, f_y)| \leq H_L \tag{8}$$

2) the phase response is the same

$$\measuredangle \bar{H}_t(f_x, f_y) = \measuredangle H_t(f_x, f_y). \quad (9)$$

This is accomplished by defining $\bar{H}_t(f_x, f_y)$ as follows (cf. (5):

$$\bar{H}_t(f_x, f_y) = \begin{cases} \dfrac{1}{H(f_x, f_y)}, & \text{for } \dfrac{1}{|H(f_x, f_y)|} \leqslant H_L \quad (10) \\ H_L + j0, & \text{for } |H(f_x, f_y)| = 0 \quad (11) \\ H_L \dfrac{\text{Re}\,[H(f_x, f_y)] - j\,Im\,[H(f_x, f_y)]}{H(f_x, f_y)}, & \\ & \text{for } \dfrac{1}{|H(f_x, f_y)|} > H_L. \quad (12) \end{cases}$$

Equations (10), (11), and (12) are consistent with (8) and (9); that is the phase response is preserved and the dynamic range of the magnitude response can be controlled with the parameter H to prevent noise amplification and/or overflow of computer registers. In a digital computer all these operations are straightforward and we have coded them in Fortran routines [3]. Examples of applications are given in Section IV. It should be noted that under the transformation (10)-(12) a real PSF remains real, and an even PSF remains even.

Since the system transfer function usually has a low-pass characteristic, the inverse filter has a high-pass characteristic. Therefore, it is convenient to cascade the inverse filter with a low-pass filter to reduce the noise at high frequencies where the gain of the inverse filter is greatest. The choice of the cutoff frequency of the low-pass filter is a tradeoff between the desired resolution and noise.

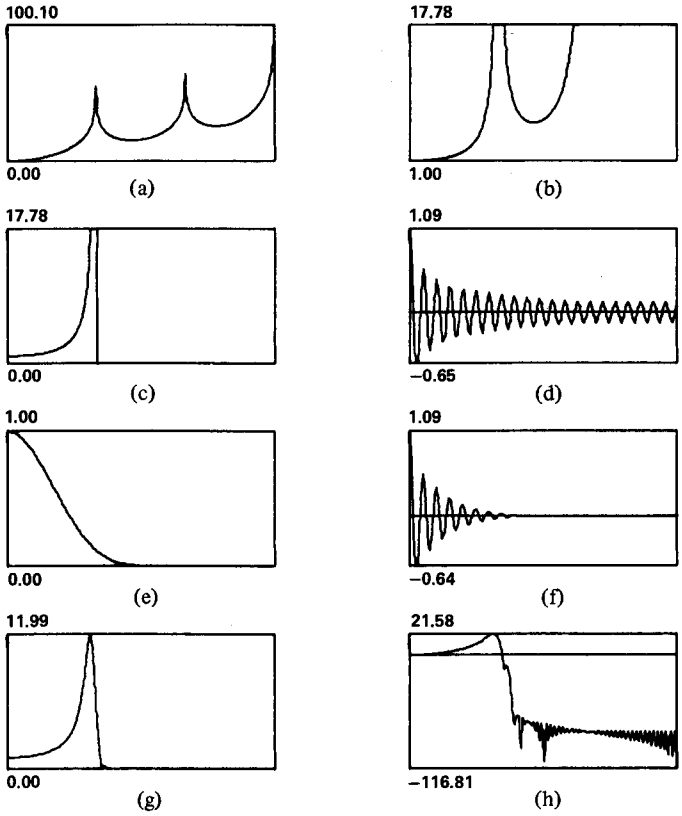

Fig. 6. Plots of relevant functions in the design of a digital tomographic filter using the windowing technique. (a) Ideal inverse filter (in dB). (b) Inverse filter with hard-limited magnitude response. (c) The filter in (b) cascaded with an ideal low-pass filter. (d) Impulse response of the filter in (c). (e) Kaiser window with $\beta = 9$. (f) Windowed impulse response. (g) Magnitude response of the tomographic filter. (h) Same as (g) in dB.

C. Determination of the Digital Filter Coefficients

During this research the windowing technique for designing two-dimensional FIR filters was chosen because it can easily be used to approximate a completely arbitrary complex frequency response, such as that of a tomographic filter as given in (5). This includes both the magnitude and the phase because the information carried by the phase is very important when dealing with images. The argument justifying the use of the windowing technique is similar to that for the use of inverse filtering. During this research the parameters of the tomographic filters were changed frequently, thus a simple design technique was justified for this initial research. In future work, optimized two-dimensional IIR filters may prove more adequate.

The process of determining the digital filter coefficients can be described with reference to Fig. 6. This figure shows one-dimensional functions only, because the two-dimensional filters used were separable. Nevertheless, the same procedure would apply to nonseparable filters because the extension of the windowing technique to two dimensions is straightforward. Fig. 6(a) shows the magnitude response of the ideal inverse filter, as per (5). During this step a correction by interpolation may be included, if the sampling intervals of the PSF $h(x, y)$ are not equal to those of the digitized radiograph. From the plot in Fig. 6(a) a suitable hard-limit is chosen and by applying the transformations (12) the filter in Fig. 6(b) is obtained. During this research the hard-limits were selected by trial and error; however, they could eventually be determined for each given system in order to produce optimum results. Fig. 6(c) shows the effect of introducing a low-pass filter to reduce the noise at high frequencies as previously discussed. Fig. 6(d) shows the impulse response of this filter. The windowing technique can now be applied to determine the digital filter coefficients. The Kaiser window [13] was chosen, not only because of its optimal behavior[6], but also because it contains a parameter β that controls the frequency response tradeoff between resolution and ripple.

A high β, such as $\beta = 9$, was used in order to obtain low ripples and a smooth transition band. Fig. 6(f) shows the result of multiplying the impulse response in Fig. 6(d) by the Kaiser window in Fig. 6(e). Finally, the FFT is used to obtain the coefficients of the tomographic filter in a form suitable for fast convolution realizations. The magnitude response of the tomographic filter is shown in Fig. 6(g) and (h). An example of a tomographic filter that was actually used is shown in Fig. 7. This filter was obtained by multiplying two one-dimensional digital filters. Source listings of the computer programs (Fortran) used throughout this research can be found in [7][7].

[6]In the sense that it is a finite duration sequence that has the minimum spectral energy beyond some spectral frequency.

[7]These include X-ray image formation simulator, filter design and implementation, and very fast two-dimensional Fourier transform programs.

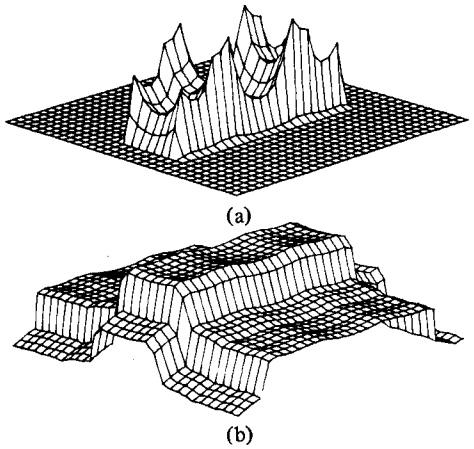

Fig. 7. Typical tomographic filter. (a) Magnitude response. (b) Magnitude response in dB.

IV. Implementation of Tomographic Filters

Filtering the data is the simplest operation in the whole process, although it is the one that requires the most CPU time. A portion of the radiograph to be processed is chosen and multiplied by a two-dimensional cosine taper data window to reduce the effects of leakage. It is then Fourier transformed using a two-dimensional FFT. The size 256 X 256 was found to give a good tradeoff between resolution and cost for these experiments. The transform of the radiograph and the filter coefficients are complex multiplied point-by-point. The result is inverse transformed, quantized to 6 bits and it is stored ready for display.

Three types of experiments were carried out to evaluate practically the performance of tomographic filters. For the first two, the radiologic system was simulated in a digital computer by approximating the image formation equations in the space domain [3]. This approach provided flexibility in the choice of focal spot shapes and object characteristics. Two types of objects were simulated: "thin" objects (single layer) and a three-dimensional object composed of only 2 layers at different depths. Pictorial results of these simulations are reported below. The third type of experiment used actual radiographs. The radiographs were digitized and the impulse response was calculated, as previously discussed. The discussion of the results in each case follow.

A. Experiments with Thin Objects (Simulated Radiographs)

Fig. 8 shows the results of using tomographic filters designed for various depths. The focal spot intensity distribution used was

$$I_o(x,y) = \exp\{-2(x^2+y^2)\} \quad -1.4 < x,y < 1.4. \quad (13)$$

The tomographic filters had a magnitude hard-limit of $H_L = 40$ dB and a cutoff frequency of $f_c = 1.25$ cycles/mm. This cutoff frequency was found to be appropriate for this type of images. The sharpest image is obtained when the tomographic filter is designed for the depth where the thin object is located [Fig. 8 (f)]. When the object is between the plane of cut of the tomographic filter and the film [Fig. 8(b) and (c)], the effects of a high-pass filter are clearly manifest, especially in Fig. 8(b). On the other hand, when the object is between the plane of cut and the focal spot [Fig. 8(g)] the low-pass characteristics of the overall transfer function are evident.

B. Experiments with Thick Objects (Simulated Radiographs)

To observe the effect of layer superpositions, with the tomographic filter acting simultaneously on all layers, a three-dimensional object was composed by having a part of a star test pattern at one level and another part at a different level, with the bar structures oriented at 90°, with respect to one another. Fig. 9 shows the simulated radiographs with different focal spots. The uniform-square focal spot had dimensions of 2 X 2 mm. The Gaussian focal spot is defined in (13). The focal spot to film distance is 1000 mm and the two layers of the object are positioned at depths (distance from the film) of 400 mm (layer 1) and 600 mm (layer 2). The absorption in the object was always 100 percent except for Fig. 9(c) in which it was 50 percent.

Fig. 9(d) shows a simulation of an X-ray image obtained with a punctual focal spot. It has a block-like structure, not visible in the other simulated radiographs because it is smeared out by the blur. This block-like nature is due to the magnification of the sampling intervals in the object (about 0.25 mm) when they are projected on the film plane. This effect would have been minimized by using sampling intervals in the object equal to the sampling intervals in the film divided by the magnification factor. However, that would result in enormous computer memory requirements. On the other hand, this block-like structure is advantageous in these tests, because it permits the evaluation of the recovery of small details with tomographic filters.

Fig. 10 shows the two-dimensional Fourier transforms of the simulated radiographs in Fig. 9. The characteristics of the focal spot are also manifested in Fig. 10. For example, the lobes of a sampling function may be seen in Fig. 10(a) along each axis.

Tomographic filters were designed as discussed previously. The impulse response had 129 X 129 samples and the number of samples to be processed was 128 X 128, which results in two-dimensional transforms of size 256 X 256 to implement the convolution. The results of tomographic filtering are shown in Figs. 11 to 13. The characteristics of the filters used are summarized in Table I. The hard limits are cutoff frequencies were chosen here by trial and error. A discussion of the results follows.

Figs. 11 to 13 should be compared with Fig. 9(a)-(c), respectively, and Fig. 9(d) to draw the conclusions. In each case we desire to restore the sharpness of the image of one layer and degrade other images. Fig. 11 shows the results of processing Fig. 9(a) with four different tomographic filters. In Fig. 11(a) and (b) the intent is to focus on layer 2 (the one closer to the focal spot, where the magnification is higher). The restoration of layers closer to the focal spot is more difficult because they have a PSF of greater extent, and thus the zeros of its Fourier transform are closer to the origin. The difference between Fig. 11(a) and (b) is only in the filter hard-limit and cutoff frequency. In Fig. 11(c) and (d) the intent is to restore layer 1.

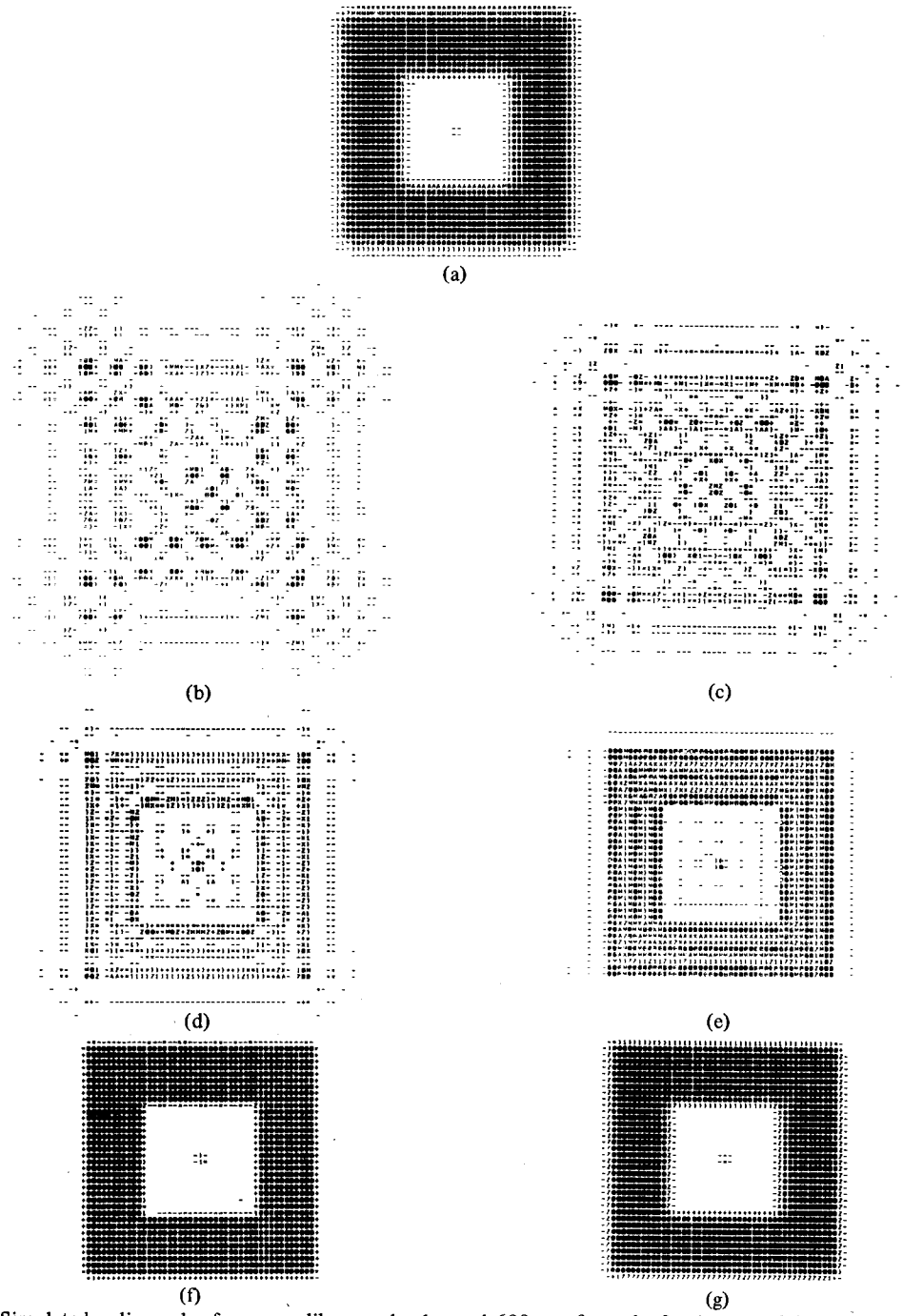

Fig. 8. (a) Simulated radiograph of a square-like annulus located 600 mm from the focal spot and 400 mm from the film. This image was processed with tomographic filters designed for layers at the following distances from the film. (b) 600 mm. (c) 550 mm. (d) 500 mm. (e) 450 mm. (f) 400 mm. (g) 350 mm.

Fig. 12 shows the results of processing Fig. 9(b) with four different tomographic filters. Since the focal spot had a Gaussian shape in this case, the problems of zeros in the Fourier transform of the PSF were not present; consequently, the cutoff frequencies of the tomographic filters were higher than for Fig. 11 (cf. Table I).

Fig. 13 shows the results of processing Fig. 9(c) with exactly the same four tomographic filters that were used to process Fig. 9(b). Here the object has 50 percent absorption instead of 100 percent as in the previous case. The 50 percent absorption more closely represents variations in an anatomical attenuation in clinical situations, which are normally of the order of 15-30 percent, especially in situations where tomography is useful. The effects of tomographic filtering are particularly good in Fig. 13(d). All the practical results discussed here are consistent with the analytical evaluations of tomographic filtering (cf. [2], [3]).

The filters used to obtain Figs. 11 to 13 did not guarantee a positive intensity output. Techniques are available to ensure positive restoration, such as homomorphic filtering [14], nu-

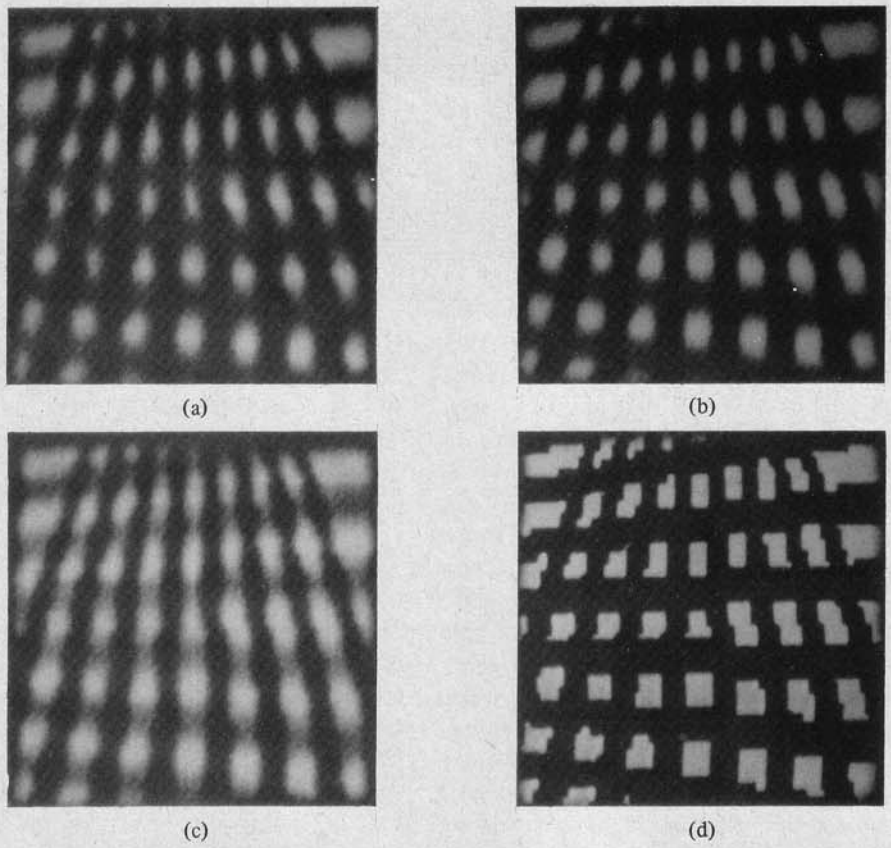

(a) (b) (c) (d)

Fig. 9. Simulated radiographs with different focal spot intensity distributions. (a) Uniform square. (b) Gaussian. (c) Gaussian (50 percent object absorption). (d) Point source.

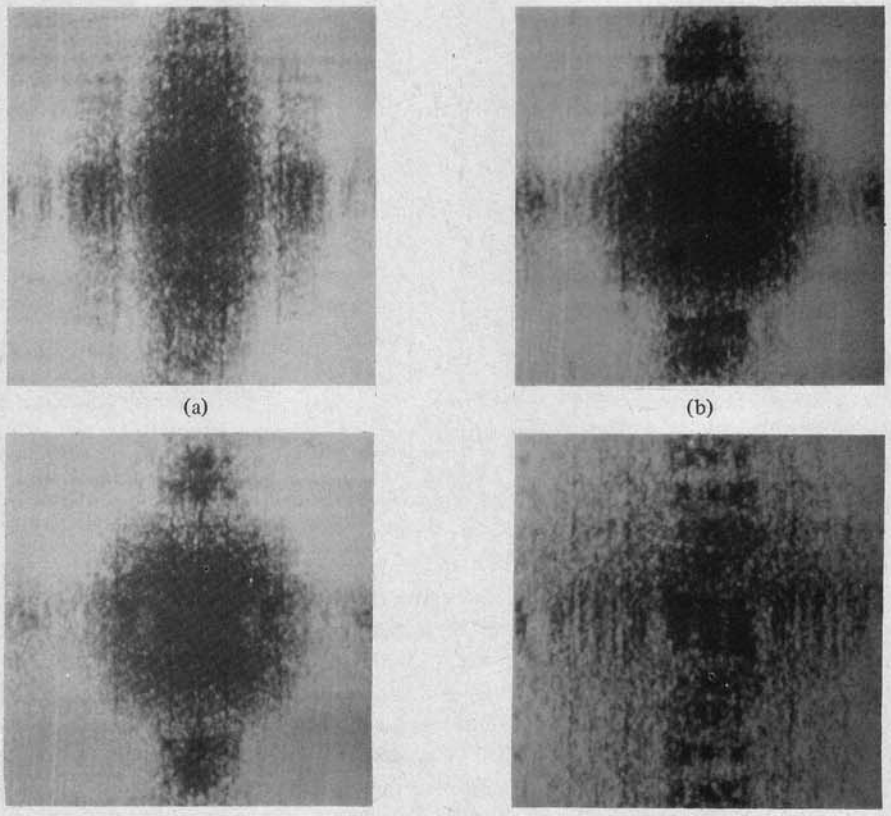

(a) (b) (c) (d)

Fig. 10. (a)–(d) Two-dimensional Fourier transform (in dB) of the radiographs in Fig. 9(a)–(d), respectively.

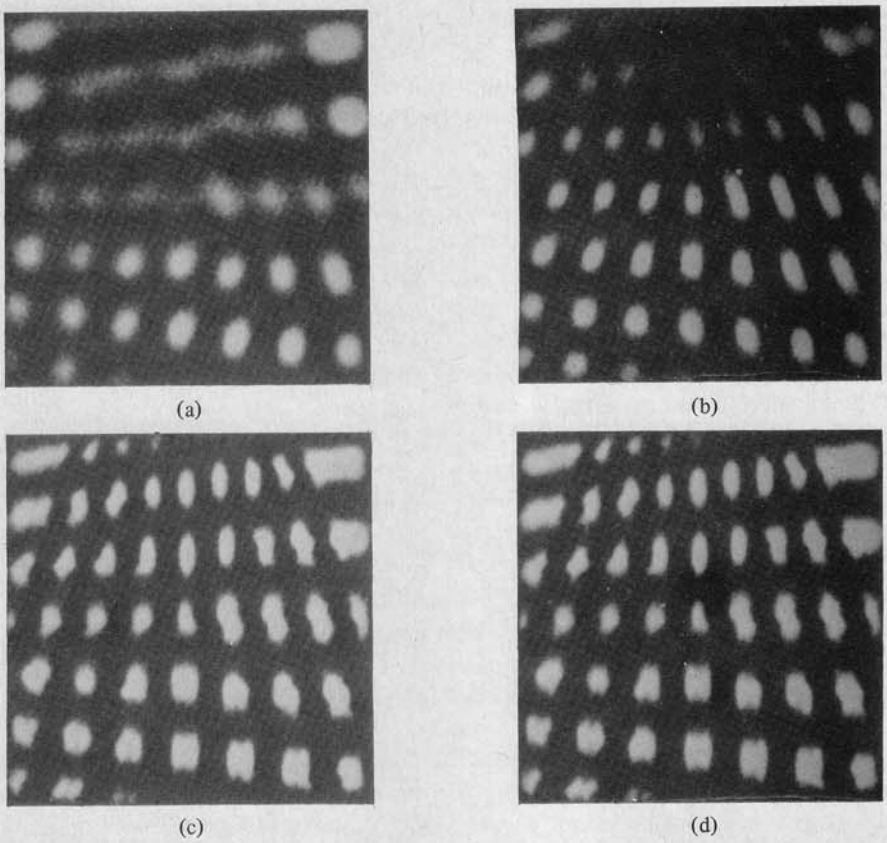

(a) (b) (c) (d)

Fig. 11. Results of filtering Fig. 9(a) with tomographic filters. For layer 2: (a) H_L = 10 dB; (b) H_L = 20 dB. For layer 1: (c) H_L = 20 dB; (d) H_L = 30 dB.

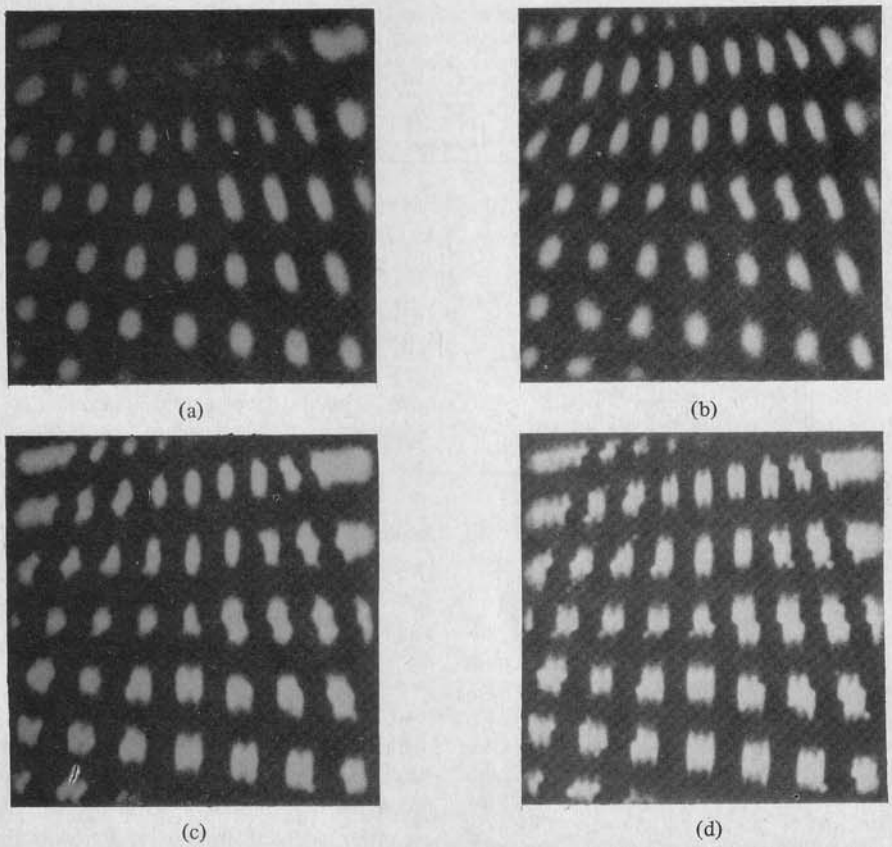

(a) (b) (c) (d)

Fig. 12. Results of filtering Fig. 9(b) with tomographic filters. For layer 2: (a) H_L = 10 dB; (b) H_L = 20 dB. For layer 1: (c) H_L = 20 dB; (d) H_L = 40 dB.

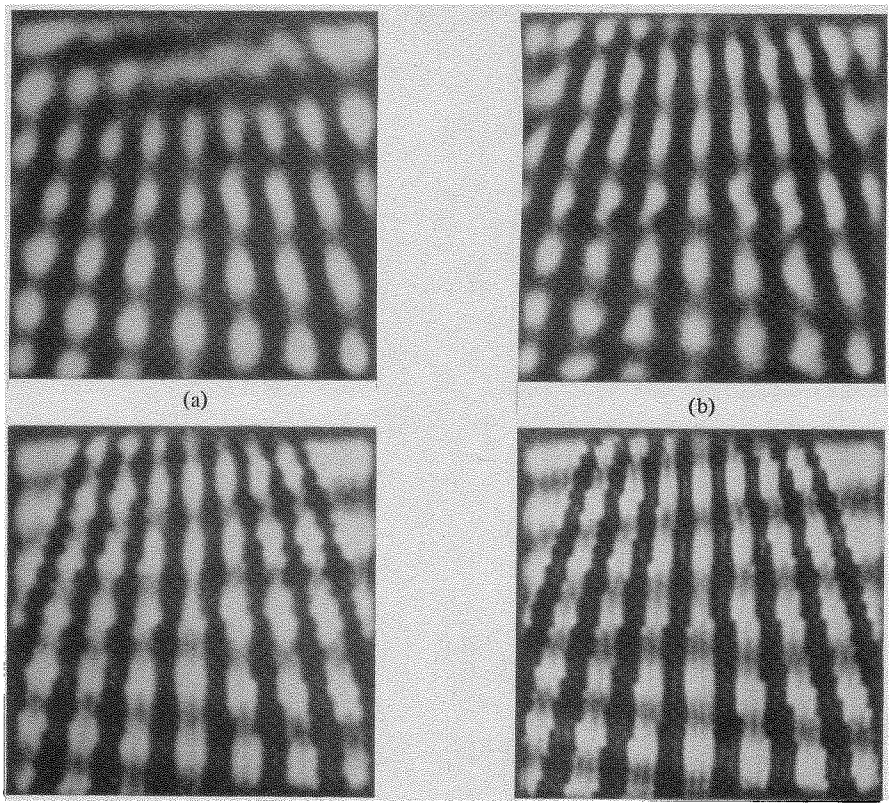

Fig. 13. Results of filtering Fig. 9(c) with tomographic filters. For layer 2: (a) H_L = 10 dB. (b) H_L = 20 dB. For layer 1: (c) H_L = 20 dB. (d) H_L = 40 dB.

TABLE I
SUMMARY OF THE CHARACTERISTICS OF THE TOMOGRAPHIC FILTERS USED TO OBTAIN FIGURES 11 TO 13

Resulting Figure	Original Figure	Focal Spot	Layer to Deblur	H_L (in dB)	Low-pass Filter Bandwidth (cycles/mm)	Nominal Blur Size (in mm)
11 (a)	9 (a)	Uniform-square	2	10	0.21	3.0
11 (b)	9 (a)	"	2	20	0.31	3.0
11 (c)	9 (a)	"	1	20	0.78	1.2
11 (d)	9 (a)	"	1	30	0.83	1.2
12 (a), 13 (a)	9 (b), 9 (c)	Gaussian	2	10	0.33	4.5
12 (b), 13 (b)	9 (b), 9 (c)	"	2	20	0.42	4.5
12 (c), 13 (c)	9 (b), 9 (c)	"	1	20	0.83	2.1
12 (d), 13 (d)	9 (b), 9 (c)	"	1	40	1.25	2.1

merical methods of image restoration [15], the Lukosz bound constraint for linear filters [15], and *a posteriori* techniques[8] [16]. In Figs. 11 to 13 the negative intensities were clipped away. After the reconstruction with a tomographic filter, enhancement techniques can be used to produce radiographic images more appealing or more informative to the eye. These techniques were not used to produce Figs. 11 to 13, so that the raw results of tomographic filtering could be appreciated better. An overview of image enhancement techniques can be found in [17].

[8]The *a posteriori* techniques that have been suggested to deal with negative intensities are the following: 1) take the absolute value, 2) take the square, 3) add a constant, and 4) clip at zero and neglect negative intensities. All these operations are nonlinear and increase the bandwidth of the result [16].

C. Experiments with Actual Radiographs

In order to test the performance of digital tomographic filters with actual radiographs, a number of radiographs of a mock chest (phantom), with a different set of lesions situated on either side of the chest, were obtained. However, due to computer memory limitations, only small areas of about 50 X

50 mm^2 could be digitized and processed. These subimages contained two lesions, one on either side of the chest. Since the small size of these subimages do not make the results conclusive, illustrations are not included here, but they can be found in [3]. In general, the results showed that, after processing with tomographic filters, the image of a lesion is smeared in the background when the depth of the lesion and that of the tomographic filter do not match.

More work is required to determine specific medical applications of tomographic filtering. The size and shape and distribution of structures in the object, together with the properties of tomographic filtering, will determine the applications of tomographic filtering. With uniform absorption objects (low frequencies) tomographic filtering does not help in differenciating among layers. To do tomographic filtering, structures with edges are needed (high frequency components). Fortunately, in radiologic applications there is interest in small objects such as lesions, blood vessels, etc. Even when these objects are readily seen in the form of a white spot or line on the film, some help is needed in their interpretation (e.g., to find their position in the depth of the object).

Finally, another factor that affects the quality of filtered radiographs is the ripples in the impulse response for the layers on the side of the film when the plane of cut is close to the focal spot. In some cases this is an advantage if it causes unwanted details to disappear from overlaying layers, but on the other hand the ripples may lead to false interpretations.

A possible approach to learn how to deal with all these factors which depend on the (unknown) object is to do a series of filtrations of the same radiograph starting with "harmless" tomographic filters, whose transfer function is close to unity and continuing processing with more "aggressive" tomographic filters, until the image is dominated by noise. This series can be repeated for different depths. By comparing the successive outputs like in a movie, the changes in the structures can be examined in detail. Of course, doing this on a routine basis may not be practical but it could be useful in future experiments with tomographic filters. This technique could also be applied in certain cases when a new radiograph cannot be obtained or a better radiologic technique is not available (e.g., old radiographs from archives, remote diagnosis, etc.).

Tomographic filters could easily be applied when on-line image processing and communication systems [18] are available in hospitals, thus facilitating the storage, retrieval, processing, and display of the images.

V. Conclusions

In this paper we have shown how to design and implement digital tomographic filters for radiographs. The technique presented uses hard limits and cutoff frequencies to prevent noise amplification. The windowing method is used to determine the filter coefficients. Tomographic filters were tested with simulated radiographs and actual radiographs. The results are consistent with analytical evaluations of tomographic filtering (cf. [2]). These theoretical and practical evaluations of the performance of tomographic filters have shown that the image quality results cannot be as good as those of standard tomography or three-dimensional radiographic (multiprojection) reconstruction techniques in terms of the thickness of the tomographic layer but they represent an improvement over conventional radiology. Tomographic filters allow the image analyst to interact with the system to exploit its capabilities, rather than being a passive observer of an image. They have the advantage in that they can be implemented without the use of any special-purpose X-ray hardware. Finally, while other tomographic procedures use moving parts during the exposure and depend on multiple exposure to obtain additional information from a patient's body, with the consequent increase in radiation dose, tomographic filters use instead multiple filtrations of a single radiograph, without endangering the patient.

More research is required to determine possible clinical applications of tomographic filtering as well as to optimize their design and implementation. A few possible directions follow. Since the performance of tomographic filtering depends on the characteristics of the human body, such as position and size of lesions, overlaying structures (e.g., ribs), exposure, geometry, direction of the projection, etc., the medical evaluation of tomographic filtering should take into account these variables in order to find out for what applications (e.g., type of disease, organ, lesions) tomographic filtering could complement other methods in the medical imaging hierarchy. Medical image information quality standards are needed so that the results of experiments can be judged accordingly and rules can be set for calibration of experiments. The peculiarities of the tomographic filtering process, such as the high-pass effect between the plane of cut and the film, need to be investigated more with respect to the diagnostic quality of the processed radiograph. The influence of the type of focal spot [i.e., the exposure function $I_o(x_o, y_o)$] could also be investigated taking into account the tradeoffs, e.g., larger focal spots give better depth resolution but restoration is more difficult.

Another area is the design of digital tomographic filters. Filter structures, such as homomorphic, Wiener, and various modifications of inverse filtering, could be evaluated to determine their suitability and preference for tomographic filtering. The use of recursive techniques for digital tomographic filters could be investigated because "recursive tomographic filters" would probably use less computer memory and time in their implementation. Filter parameters such as the order of the tomographic filter, computer wordlength, mode of arithmetic, and roundoff errors would influence both the cost and the quality of the results, thus tradeoffs should be determined.

Finally, extensions of this research can be suggested. It might be possible to identify the blur characteristics from the radiograph itself, using the techniques of power spectrum and power cepstrum estimation. The use of tomographic filtering might be useful as a preprocessing technique for automated pattern recognition processes. Tomographic filtering may also have applications in standard tomography, in order to change the plane of cut of a tomogram by means of tomographic filtering. The tomographic filtering concept might be useful in other areas such as geophysics, astronomy, and image analysis.

REFERENCES

[1] J. M. Costa, A. N. Venetsanopoulos, and M. Trefler, "Digital tomographic filtering of radiographs," this issue, pp. 76-88.

[2] —, "Evaluation of digital tomographic filters," Dep. Elec. Eng., Univ. Toronto, Ont., Canada, Communications Tech. Rep., 1983.

[3] J. M. Costa, "Design and realization of digital tomographic filters for radiographs," Ph.D. dissertation, Univ. Toronto, Ont., Canada, 1981.

[4] J. M. Costa and A. N. Venetsanopoulos, "Digital tomographic restoration of radiographs," in *Proc. Conf. Digital Processing of Signals in Commun.*, Univ. Technology, Loughborough, England, Sept. 1977, IERE Conf. Proc. no. 37, pp. 559-567.

[5] J. M. Costa, "Tomographic filters for digital radiography," *Digital Radiography*, Proc. SPIE 314, pp. 66-71, 1981.

[6] —, "Insight into radiological images," in *Proc. 1st I.A.S.T.E.D. Symp. Applied Informatics*, Lille, France, Mar. 15-17 1983, vol. I, pp. 189-192.

[7] J. B. Minkoff, S. K. Hilal, W. F. Konig, M. Arm, and L. B. Lampert, "Optical filtering to compensate for degradation of radiographic images produced by extended sources," *Appl. Opt.*, vol. 7, no. 4, pp. 633-641, 1968.

[8] G. A. Krusos, "The amelioration of contrast and resolution of X-ray images using optical signal processing," Eng. Sc.D. dissertation, Columbia Univ., New York, 1971.

[9] R. M. Mersereau and A. V. Oppenheim, "Digital reconstruction of multidimensional signals from their projections," *Proc. IEEE*, vol. 62, pp. 1319-1338, 1974.

[10] H. C. Andrews, "Digital image restoration: A survey," *Computer (Special Issue on Digital Image Processing)*, vol. 7, no. 5, pp. 36-45, May 1974.

[11] H. C. Andrews and B. R. Hunt, *Digital Image Restoration.* Englewood Cliffs, NJ. Prentice-Hall, 1977.

[12] B. R. Hunt and H. C. Andrews, "Comparison of different filter structures for image restoration," in *Proc. 6th Annu. Hawaii Int. Conf. Systems Sci.*, Jan. 1973.

[13] J. F. Kaiser, "Nonrecursive digital filter design using the I_0-sinh window function," in *Proc. 1974 IEEE Symp. Circuits Syst.*, Apr. 22-25, 1974, pp. 20-23.

[14] T. G. Stockham, Jr., "Image processing in the context of a visual model," *Proc. IEEE (Special Issue on Digital Picture Processing)*, vol. 60, pp. 828-842, July 1972.

[15] H. C. Andrews, "Positive digital image restoration techniques—A survey," Aerospace Corporation, Tech. Rep. No. ATR-73 (8139)-2, Feb. 25 1973.

[16] T. S. Huang, Ed., *Picture Processing and Digital Filtering.* New York: Springer-Verlag, 1975.

[17] H. C. Andrews, "Monochrome digital image enhancement," *Appl. Opt.*, vol. 15, no. 2, pp. 495-503, Feb. 1976.

[18] J. M. Costa, "Medical image communication systems," *Digital Radiography*, Proc. SPIE 314, pp. 380-388, 1981.